Operating conditions for attenuating Ni/La_2O_3-αAl_2O_3 catalyst deactivation in the steam reforming of bio-oil aqueous fraction

Aingeru Remiro, Beatriz Valle*, A.T. Aguayo, Javier Bilbao, Ana G. Gayubo

Chemical Engineering Department, University of the Basque Country

P. O. Box 644, 48080, Bilbao, Spain. Phone: +34 946 015361. Fax: +34 946 013 500.
**Email: beatriz.valle@ehu.es*

Abstract

A study was carried out on the effect of temperature (in the 500-800 ºC range) and space-time (between 0.10 and 0.45 $g_{catalyst}h(g_{bio\text{-}oil})^{-1}$) on Ni/$La_2O_3$-α$Al_2O_3$ catalyst deactivation by coke deposition in the steam reforming of bio-oil aqueous fraction. The experiments were conducted in a two-step system, provided with a thermal step at 200 ºC for the pyrolytic lignin retention and an on-line step of catalytic reforming in fluidized bed reactor. Full bio-oil conversion and a hydrogen yield of around 95 % (constant for 5 h) were achieved at 700 ºC, S/C (steam/carbon) ratio of 12 and space-time of 0.45 $g_{catalyst}h(g_{bio\text{-}oil})^{-1}$. The results of catalyst deactivation were explained by mechanisms of coke formation and evolution, which are established based on kinetic results and coke analysis by temperature programmed combustion. At 700 °C the coke is gasified and Ni does not undergo sintering. The results of hydrogen yield were compared with those obtained in the literature using different reaction technologies.

Keywords: Steam reforming, Bio-oil, Hydrogen, Deactivation, Ni/La_2O_3-αAl_2O_3 catalyst, Coke.

1. Introduction

Hydrogen is an emerging clean energy carrier and an important chemical raw material for oil refineries, ammonia production, methanol synthesis and other minor applications, such as electronics, food industry and metallurgy. The current world consumption of hydrogen has a sustained annual growth forecast of 5-10 % (corresponding to 50 % of the total energy consumption predicted for 2100) [1,2].

Currently hydrogen is mainly obtained from fossil fuels by steam reforming (48 % from natural gas, 30 % from oil-derived naphthas and 18 % from coal) [3], which results in CO_2 emissions during its production processes. The future hydrogen market, as fuel and energy carrier, is promoted by the need for reducing CO_2 emissions, which requires its production from renewable raw materials and energy sources. Consequently, the forecast until 2100, establishes a transitional scenario from the production of hydrogen from fossil fuels and from water (by electrolysis), in which the emerging raw material is the lignocellulosic biomass, due to its availability and renewable nature [1-3].

Hydrogen can be generated from biomass on a large scale by thermochemical processes, such as high temperature and catalytic pyrolysis [4] and gasification [5,6]. Flash pyrolysis followed by steam reforming of the pyrolysis oil (bio-oil) is one of the most promising routes, based on the possibility of geographic relocation of the biomass pyrolysis plants (with simple technology, of low-cost and environmentally friendly) [7], with subsequent bio-oil transportation and with reforming centralized at large-scale.

The oxygenated organic compounds in the bio-oil can be simply represented with a $C_nH_mO_k$ chemical formula and their steam reforming can be described according to the following reactions:

$$C_nH_mO_k + (n\text{-}k)\ H_2O \rightarrow nCO + \left(n + \frac{m}{2} - k\right)H_2 \quad (1)$$

The above reaction is followed by the water-gas-shift reaction (WGS):

$$CO + H_2O \Leftrightarrow CO_2 + H_2 \quad (2)$$

Thus the overall steam reforming reaction can be represented as follows:

$$C_nH_mO_k + (2n\text{-}k)H_2O \Leftrightarrow nCO_2 + \left(2n + \frac{m}{2} - k\right)H_2 \quad (3)$$

Nevertheless, crude bio-oil has a composition and properties that hinder its catalytic reforming. It is a remarkable fact that the derivatives obtained by pyrolysis of the lignin contained in the biomass, tend to re-polymerize with the heating required for their vaporization, which results in the formation of a carbonaceous deposit (pyrolytic lignin). This deposition creates problems that affect the reactor feed system and operation, and causes catalyst deactivation.

With the addition of water, bio-oil can be separated into a hydrophobic lignin-derived fraction and an aqueous (hydrophilic) fraction that contains mostly carbohydrate-derived compounds. This aqueous fraction, with lower content of phenolic compounds derived from the pyrolysis of lignin, can be reformed with less pyrolytic lignin deposition during its vaporization than that corresponding to crude bio-oil vaporization [8]. In addition, the feed of this aqueous fraction of bio-oil reduces the need for co-feeding water co-feeding for the steam reforming reaction.

Early studies on reforming the aqueous fraction of bio-oil were performed in a fixed bed [9], by using bio-oil fraction with high water content, which attenuates catalyst deactivation [10]. Bed blocking problems were observed and mitigated by the use of fluidized bed reactors [11-13]. Kechagiopoulos et al. [14] and Basagianis and Verykios [15] emphasized the operational difficulties due to a thermal coke deposition on the reactor walls, which led to the use of spouted bed reactors [16]. van Rossum et al. [17] used a two-stage reactor concept, which consisted of a sand fluidized bed for a thermal pre-treatment, followed by a catalytic fixed bed. The catalysts used in those studies were based on Ni, such as commercial catalysts for naphtha reforming [9,18], Ni/Al_2O_3 modified by Ca or Mg [12], Ni/dolomite [11] and Ni/MgO [13]. Catalysts based on noble metals were also used, such as $Ru\text{-}Mg\text{-}Al_2O_3$ supported in monoliths, porous ceramic materials and $\gamma\text{-}Al_2O_3$ [15]. The standard hydrogen yield obtained was 65 %, at temperature of around 800 °C with S/C (steam-to-carbon ratio) greater than 10 and space velocity of around WHSV = 1.0 h^{-1}. Gasification of coke is enhanced by increasing temperature and S/C and thereby catalyst deactivation is attenuated. Yan et al. [19] studied the incorporation of CO_2 sorbents along

with a commercial catalyst (not described) and they attained higher hydrogen yield with calcined dolomite (up to 83 %) and CaO (up to 85 %) than without sorbent (75 %).

The present work delves into the steam reforming of the aqueous fraction of a bio-oil obtained by flash pyrolysis of pine sawdust over Ni/La_2O_3-αAl_2O_3 catalyst. The addition of La_2O_3 to Ni/αAl_2O catalyst improves notably its stability since it attenuates deactivation by coke deposition and metal sintering [20]. The reaction system consists of two steps on-line (thermal and catalytic) which enables continuous operation (Fig. 1). The vaporized bio-oil flows in a pipeline, at 200 °C, in which certain bio-oil components (mostly those derived from lignin pyrolysis) re-polymerize and the remaining volatiles are reformed on-line in a fluidized bed reactor that contains the catalyst. The main objective of this study is to establish the most suitable range of operating conditions for obtaining a high and steady hydrogen yield. Accordingly, the effect of operating conditions on the catalyst coke deposition was studied and the coke was analyzed by temperature programmed combustion (TPO). The results were explained by the effect of operating conditions on the mechanisms of coke formation, evolution and gasification.

Figure 1

2. Experimental

2.1. Bio-oil

The bio-oil used in this paper was obtained by flash pyrolysis of pine sawdust in a semi-industrial demonstration plant, located in Ikerlan-IK4 technology center (Alava, Spain), with the biomass feeding capacity of 25 kg/h [21]. This plant was developed based on previous results obtained in a laboratory plant (120 g/h) at the University of the Basque Country [22,23]. The aqueous fraction was obtained by phase separation after adding water to crude bio-oil, in water/bio-oil mass ratio= 2/1, by following the procedure described by Czernik et al. [18]. The composition of the crude bio-oil and the corresponding aqueous fraction were determined by GC/MS analyser (*Shimadzu QP2010S device*) and they are shown in Table 1, on a water-free basis. Their corresponding molecular formulas are $C_{4.3}H_{7.2}O_{2.6}$ and $C_{4.1}H_{7.4}O_{2.7}$ for the crude bio-oil and its aqueous fraction, respectively. Correct and complete characterization of bio-oil is a difficult task that requires the

combination of results from several analytical techniques. The CHO formula obtained by GC/MS was confirmed by elemental analysis (*Leco CHN-932 analyzer* and ultra-microbalance *Sartorious M2P*), with similar results, although less reproducible.

Table 1

2.2. Catalyst synthesis and properties

The Ni/La_2O_3-αAl_2O_3 catalyst was prepared with the method described by Alberton et al. [20,24]. The La_2O_3-αAl_2O_3 support was obtained by impregnation of α-Al_2O_3, under vacuum at 70 °C, with aqueous solution of $La(NO_3)_3.6H_2O$ (*Alfa Aesar, 99%*), followed by drying at 100 °C for 24 h and calcination at 900 °C for 3 h. After subsequent impregnation with $Ni(NO_3)_2.6H_2O$ and drying at 110 °C for 24 h, the final calcination was carried out at 700 °C for 3 h.

The physical properties of this catalyst, such as BET surface area (37.6 m^2/g), pore volume (0.145 cm^3/g) and average pore size (11.9 nm) were evaluated from N_2 adsorption-desorption isotherms, obtained by using a *Micromeritics ASAP 2010C* analyzer. This device is also used for hydrogen chemisorption measurements for quantifying Ni dispersion and specific metallic surface, with the resulting values of 1.9 % and 12.4 m^2/g_{metal}, respectively.

Temperature programmed reduction (TPR) measurements were conducted on an *AutoChem II 2920 Micromeritics* and the TPR-profile of this catalyst showed a high proportion of $NiAl_2O_4$ spinel phase (characteristic peak at 650-676 °C) [25] due to a strong interaction between Ni and La ions, which is consistent with the findings of Sanchez-Sanchez et al. [26]. Nickel content (9.92 wt %) was measured by inductively coupled plasma and atomic emission spectroscopy (ICP-AES). The X-ray diffraction (XRD) pattern measured on a *Bruker D8 Advance* diffractrometer with a $CuK_{\alpha 1}$ radiation showed diffraction lines corresponding to the reflection of Al_2O_3 phase and Ni^0 phase (at 2θ angle of 44.5º, 51.9º and 76.4º). $LaAlO_3$ phase (La_2O_3 combined with α-Al_2O_3) is also detected [20].

The TPO (temperature programmed oxidation) analyses of the coke deposited on deactivated catalysts were conducted by combustion with air in a *Setaram TG-DSC-11*

Calorimeter coupled to a mass spectrometer *Thermostar Balzers Instrument* for monitoring the signals corresponding to mass 18 (H_2O), and 44 (CO_2).

2.3. Reaction equipment and operating conditions

The reaction equipment has been previously described in detail for the transformation of bio-oil and bio-oil+methanol into hydrocarbons [27] and it consists of two reactors on-line (Fig. 2). The first reactor (thermal processing of bio-oil) retains the carbonaceous solid (pyrolytic lignin) formed by re-polymerization of certain bio-oil oxygenated components. The volatile compounds leaving this thermal step are subsequently transformed (by catalytic steam reforming) in the second unit (fluidized bed reactor). The controlled deposition of pyrolytic lignin in a specific thermal step prior to the catalytic reactor minimizes the operating problems caused by this deposition and attenuates catalyst deactivation. This fact was previously verified for the catalytic conversion of crude bio-oil into hydrocarbons [28,29].

The on-line analysis of the reforming products is carried out continuously (more representative and steady than discontinuous sampling) with a gas chromatograph (*Agilent Micro GC 3000*) provided with four modules for the analysis of: (1) permanent gases (O_2, H_2, CO, and CH_4) with 5A molecular sieve capillary column; (2) light oxygenates (C_{2-}), CO_2 and water, with Plot Q capillary column; (3) C_2-C_4 hydrocarbons, with alumina capillary column; (4) oxygenated compounds (C_{2+}) with Stabilwax type column.

Figure 2

The experimental two-unit system was operated at atmospheric pressure and the bio-oil aqueous fraction feeding rate (0.1 ml/min) was controlled by an injection pump *Harvard Apparatus 22*. The particle size of the catalyst was 150-250 μm and it was mixed with a solid inert (carborundum, 37 μm) in catalyst/inert mass ratio of 4/1 for improving the fluid-dynamic properties of the catalytic bed. Prior to the reforming reactions, the catalyst was reduced at 700 ºC for 2 h by using H_2-He flow (5 vol % of H_2). The reforming conditions were: thermal step, 200 ºC; catalytic steam reforming, 500-800 ºC; steam-to-carbon ratio (steam/carbon ratio in bio-oil) at fluidized bed reactor inlet (S/C) = 12; space-time (τ) = 0.10-0.45 $g_{catalyst}$ h $(g_{bio\text{-}oil})^{-1}$; $G_{C1}HSV$= 8100-40300 h^{-1} (calculated in CH_4 equivalent

units).

3. Results and discussion

3.1. Reaction indices

Steam reforming of the aqueous fraction of bio-oil, with $C_{4.1}H_{7.4}O_{2.7}$ as elemental composition and steam to carbon ratio (S/C) of 7, proceeds according to oxygenates reforming reaction (Eq. 3). The yield of pyrolytic lignin deposited in the thermal treatment step at 200 ºC was 30 wt% (referred to bio-oil oxygenated compounds) and the resulting composition of the bio-oil that enters the catalytic reactor is $C_{3.7}H_{8.4}O_{2.9}$. Considering this composition and the water content, the resulting S/C ratio is 12. Consequently, the steam reforming reaction stoichiometry is:

$$CH_{2.27}O_{0.78} + 1.22\ H_2O \rightarrow CO_2 + 2.35\ H_2 \quad (4)$$

Therefore, the maximum yield of H_2 that can be obtained from this feed is 2.35 moles of H_2/mol of C fed.

The aforementioned high value of S/C (12) is consequence of the addition of water in the separation treatment of the aqueous fraction of bio-oil (with water/bio-oil ratio of 2/1). Previous experimental results (not shown here) proved that for S/C ratios higher than 8, the H_2 yield is maximum. Consequently, this water content in the aqueous fraction is suitable for the steam reforming.

Bio-oil conversion is calculated from oxygenates molar flowrates at inlet and outlet (unreacted bio-oil) of the catalytic reactor, according to:

$$X = \frac{F_{\text{bio-oil,inlet}} - F_{\text{bio-oil,outlet}}}{F_{\text{bio-oil,inlet}}} \quad (5)$$

The bio-oil molar flowrate at catalytic reactor inlet ($F_{\text{bio-oil,inlet}}$) is calculated from the mass flowrate of the bio-oil fed to the system and its $C_nH_mO_k$ empirical formula (calculated by GC/MS analysis). After the thermal treatment step, the molecular formula of the bio-oil that enters the reactor is recalculated by subtracting the pyrolytic lignin deposited in this unit. For this purpose, the pyrolytic lignin deposition rate and its elemental composition (C, H, and O) were considered.

The bio-oil molar flowrate at reactor outlet ($F_{bio\text{-}oil,outlet}$) is calculated from the molar fraction of oxygenates (analyzed by microGC and by GC/MS) and the total number of moles at the reactor outlet, determined by mass balance for the catalytic reactor.

The hydrogen yield is calculated as a percentage of the maximum allowed by stoichiometry, which accounts for the hydrogen coming from the reactants, bio-oil and water (Eq. 4), that is 2.35 moles of H_2/mol of C fed:

$$Y_{H_2} = \frac{\text{molar flow of } H_2 \text{ obtained}}{(2n + m/2 - k) \times \text{molar flow of C in the feed}} \times 100 \quad (6)$$

In practice, the yield of hydrogen is lower than the stoichiometric maximum due to undesired reactions, such as reverse WGS (Eq.2) and other secondary reactions (thermal decomposition, methanation, etc.).

The yield of each carbon-containing byproduct (CO, CO_2 and CH_4 and light hydrocarbons C_2-C_4) is quantified:

$$Y_i = \frac{\text{molar flow of i } (CO, CO_2, CH_4, HCs) \text{ obtained}}{\text{molar flow of C in the feed}} \times 100 \quad (7)$$

The selectivity of each *i* product is calculated as the percentage of each component in the product stream (without considering oxygenates in the bio-oil and water):

$$S_i = \frac{\text{molar flow of i obtained}}{\text{total molar flow - molar flow of (oxygenates + water)}} \times 100 \quad (8)$$

3.2. Effect of reforming conditions

3.2.1. Temperature

Fig. 3 shows the effect of reaction temperature on the evolution with time on stream of bio-oil conversion, in the 500-800 ºC range and for space-time of 0.22 $g_{catalyst}h(g_{bio\text{-}oil})^{-1}$. Full initial conversion of bio-oil is achieved above 550 ºC and catalyst deactivation is less pronounced as temperature is increased in the 500-650 °C range. Full conversion remains constant for 5 h at reaction temperatures above 700 ºC.

Figure 3

The results for the reaction product yields evolution with temperature are shown in Fig. 4, where solid lines correspond to the results at zero time on stream and dashed lines to the results at 5 h time on stream. The values for H_2 yield and selectivity are depicted in Fig. 4a and the reaction indices for the other gaseous products are shown in Fig. 4b (CO and CO_2) and Fig. 4c (CH_4 and hydrocarbons).

Figure 4

As it can be seen in Fig. 4a, initial H_2 yields higher than 90 % are obtained in the 600-800 °C range. As temperature is increased, the initial yield of CO_2 slightly decreases (Fig. 4b) and that of CO increases due to WGS reaction hindrance. Besides, the initial yield of CH_4 is of around 0.5 % throughout the temperature range studied, whereas the initial yield of light hydrocarbons is very low (Fig. 4c).

Comparison of the H_2 yield results at zero and at 5 h time on stream (Fig. 4a) evidences that it decreases slightly in the 650-700 °C range. However, this yield decreases markedly after 5 h of reaction at 500 ºC and 800 ºC (minimum and maximum temperatures of the range studied). In order to explain this result it should be pointed out the importance of temperature on the origin of catalyst deactivation [20], which is due to coke deposition below 600 ºC and to Ni sintering above 700 ºC (this will be further discussed in section 3.3 and 3.4). As the reforming activity diminishes, the CO_2 yield decreases and the CO yield increases (Fig. 4b). Cracking reactions of bio-oil oxygenates are important at 800 ºC, leading to the formation of gaseous byproducts, such as CH_4 and light hydrocarbons (Fig. 4 c).

3.2.2. Space-time

The study of space-time effect was aimed at: i) determining the minimum value required for attaining process stability, with full bio-oil conversion and constant H_2 yield with time on stream (for 5 h) and also with the need for avoiding significant formation of by-products (methane and hydrocarbons); ii) obtaining results of deactivation and catalyst samples deactivated in conditions with different concentrations of unconverted bio-oil in the reaction medium. This second objective would facilitate the understanding of the coke formation origin and it requires working with lower space-time values than for the above objective. It is beyond the scope of this paper the proposal of a kinetic model for the

transformation of bio-oil, which will require further and more detailed study of the space-time effect, with results for lower values of this variable.

Fig. 5 shows the evolution with time on stream of bio-oil conversion for different values of space-time, in the range 0.10-0.45 $g_{catalyst}h(g_{bio\text{-}oil})^{-1}$, at 700 ºC, and the results in Fig. 6 correspond to H_2 yield and selectivity (Fig. 6a), CO and CO_2 yields (Fig. 6b) and CH_4 and light hydrocarbon yields (Fig. 6c), under the same operating conditions than in Fig 5. Under these conditions, the aqueous bio-oil is almost fully converted at zero time on stream (fresh catalyst) in the whole range studied and it remains constant after 5 h of time on stream for space-time value of 0.45 $g_{catalyst}h(g_{bio\text{-}oil})^{-1}$, for which the yields of all reaction products remain also constant. For a space-time of 0.22 $g_{catalyst}h(g_{bio\text{-}oil})^{-1}$, bio-oil conversion remains constant for 5h time on stream, but there is a slight decrease in H_2 yield due to the increase of methane yield. For the lower value of space-time studied, 0.10 $g_{catalyst}h(g_{bio\text{-}oil})^{-1}$, the decrease in bio-oil conversion is noticeable from the beginning of the reaction. Moreover, H_2 yield and selectivity (Fig. 6a) and CO_2 yield (Fig. 6b) decrease continuously with time on stream, while the CO yield (Fig. 6b) and the yields of CH_4 and hydrocarbons (Fig. 6d) increase.

Figure 5

Figure 6

The aforementioned results indicate that catalyst deactivation is noticeable from zero time on stream at 0.10 $g_{catalyst}h(g_{bio\text{-}oil})^{-1}$ (Figs. 5 and 6), which notably attenuates the bio-oil reforming reaction, and the WGS reaction is also attenuated (so that CO yield increases with time on stream (Fig. 6b)). The increase with time on stream of the yields of CH_4 and hydrocarbons (to a lesser extent) may be explained by combination of two circumstances associated with deactivation: i) attenuation of oxygenate reforming reactions and, therefore, enhancement of competitive thermal cracking reactions; ii) attenuation of these by-products reforming.

Although catalyst deactivation does not affect bio-oil conversion at 0.22 $g_{catalyst}h(g_{bio\text{-}oil})^{-1}$ (Fig. 5), it does affect the products distribution, with a steady decrease in H_2 yield (Fig. 6a) and increase in methane yield (Fig. 6c).

Based on these results at 700 °C (temperature set as suitable in the previous section), a

space-time higher than 0.10 $g_{catalyst}h(g_{bio\text{-}oil})^{-1}$ is necessary for working under conditions of thermodynamic equilibrium, with H_2 yield of around 95 %. This yield is constant for at least 5 h with space-time of 0.45 $g_{catalyst}h(g_{bio\text{-}oil})^{-1}$. It is beyond the scope of this paper the long-term experiments necessary to assess the stability of the catalyst over several days.

3.2.3. Suitable range of operating conditions

An explanation of the previous results obtained in the 500-800 ºC range is provided with the scheme in Fig.7. Step 1 corresponds to the overall reforming process (Eq.1), which includes the reforming reactions of bio-oil oxygenates and the WGS reaction. Step 2 groups the reactions involving formation and development of carbonaceous structures (coke) on the catalyst (coke origin). Step 3 represents secondary reactions of oxygenates, namely, thermal decomposition, decarbonylation and methanation.

Figure 7

The results shown in sections 3.2.1 and 3.2.2 suggest that catalyst activity for the reforming reactions (step 1) diminishes with time on stream at temperatures above and below the 600-700 ºC range. This catalytic behaviour is due to coke deposition on the catalyst, which is significant at temperatures below 600 ºC (step 2) and due to catalyst deactivation by Ni sintering, which occurs above 700 °C. Consequently, competitive secondary reactions of thermal cracking (step 3) are enhanced, thus increasing the yields of CO, CH_4 and hydrocarbons with time on stream. Catalyst deactivation also attenuates the reforming reactions of these byproducts.

In order to achieve greater accuracy in the setting of suitable conditions for steam reforming, the joint effect of space-time (0.10 and 0.45 $g_{catalyst}h(g_{bio\text{-}oil})^{-1}$) and temperature (600 and 700 °C) has been analyzed. The results are shown in Fig. 8 (evolution with time on stream of bio-oil conversion), and Fig. 9 (evolution with time on stream of gaseous product yields).

Figure 8

Figure 9

Fig. 8 shows that the increase in temperature from 600 to 700 °C attenuates the decrease in bio-oil conversion with time on stream in a more pronounced way than the increase in

space-time from 0.10 to 0.45 $g_{catalyst}h(g_{bio\text{-}oil})^{-1}$. Temperature increase also attenuates the decrease in H_2 yield (Fig. 9a) and CO_2 yield (Fig. 9b) with time on stream. This effect is less noticeable for a low value of space-time (0.10 $g_{catalyst}h(g_{bio\text{-}oil})^{-1}$) when compared with the effect at a higher space-time (0.45 $g_{catalyst}h(g_{bio\text{-}oil})^{-1}$). An opposite trend is observed in the evolution with time on stream of the yields of CO (Fig. 9b), CH_4 and hydrocarbons (Fig. 9c). It is also observed that the increase in these byproduct yields with time on stream is more noticeable at 700 ºC than at 600 ºC.

These results are consistent with the hypothesis that the increase in temperature enhances secondary reactions of thermal origin (step 3 in Fig. 7) and that a low space-time (0.10 $g_{catalyst}\ h(g_{bio\text{-}oil})^{-1}$ is not enough for reforming the products of these reactions. Nevertheless, if space-time is high enough (0.45 $g_{catalyst}h(g_{bio\text{-}oil})^{-1}$) these products are transformed into H_2 and CO_2 by WGS reaction (CO) and by reforming (CH_4 and hydrocarbons).

Catalyst activity decreases with time on stream at 600 °C and 700 °C for a low space-time (Figs. 8 and 9), which evidences that a minimum space-time is required to maintain the reaction indices constant with time on stream. Based on the above results, at 700 °C and space-time of 0.45 $g_{catalyst}\ h(g_{bio\text{-}oil})^{-1}$ the catalyst reforming capacity is high enough for transforming coke precursors, and thereby for minimizing their deposition and growth on the catalyst. Accordingly, under these conditions full conversion of the aqueous bio-oil is obtained and a H_2 yield of 95 % and a H_2 selectivity of 70 % are achieved.

3.3. Deactivation of catalyst by coke deposition

3.3.1. Effect of reaction conditions

Table 2 shows the results (coke content, number of identifiable peaks and the maximum temperature of these peaks) of temperature programmed oxidation (TPO) analyses of the coke deposited on the catalyst for different reforming temperatures (experiments in section 3.2.2). Fig. 10 shows as example TPO curves of the coke deposited at 500, 550 and 650 °C.

Table 2

Figure 10

Coke contents in the 500-700 °C range are consistent with the effect of temperature on

the evolution with time of stream of reaction indices, that is, coke content decreases at higher reaction temperature. This content is 3.3 wt% at 500 °C as a result of the carbonaceous deposits formed on the catalyst due to the significant degradation that undergo the bio-oil oxygenates. At higher temperatures, the transformation of the intermediate compounds deposited into gases is enhanced, and consequently, the coke content at 700 °C is only 0.3 wt% (difficult to determine even with this technique). This low content is consequence of the pseudo-equilibrium of formation-transformation of coke precursors into gases.

The coke content of the catalyst used at 800 °C is negligible due to the reforming efficiency at this temperature and the noticeable deactivation observed (Figs. 3 and 4) is explained by the sintering of Ni (discussed later).

The coke contents obtained in this work are significantly lower compared to others reported in literature for the reforming of acetic acid (15 wt% at 750 °C with a similar catalyst [30]) and for the direct reforming of the bio-oil aqueous fraction (14.1-17.4 wt% [12]). This fact is explained by the prior step of pyrolytic lignin separation, which removes from the reaction medium a significant fraction of compounds that promote the formation of coke precursors. In addition, this previous step increases the concentration of water in the reaction medium, thus promoting gasification of coke precursors.

Fig. 11 shows the TPO curves of the coke deposited throughout the runs described in section 3.2.4 and the corresponding coke contents are shown in Table 3. In order to have better understanding of the effect of space-time on coke deposition, apart from the coke content by mass unit of catalyst, the yield of coke by mass unit of C in the feed has been given in Table 3. It is noted that coke content decreases with increasing space-time, which is consistent with the deactivation results in Figs. 8 and 9, and it is explained because the reforming of coke precursors is enhanced by increasing space-time. This effect is less evident at 700 °C due to the pseudo-equilibrium of formation-transformation of coke precursors into gases, which takes place at this high temperature.

Figure 11

Table 3

Furthermore, the number of peaks observed in the TPO curves (up to 5 at 550 °C, Table

2) and the temperature of these peaks (between 282 and 615 °C, Table 2) provide information about the heterogeneity of the coke composition (higher number of peaks in a more heterogeneous coke), and about the condensation level of coke components (higher level as peak temperature is higher). These results along with those in literature about coke deposition over reforming catalysts [12,31,32] allow establishing the hypothesis that coke is heterogeneous, with three preferential peaks (at 280-290 °C, 420 °C and 620-660 °C) that may be attributed to:

i) Coke deposited on Ni metal particles (peak at 280-290 ºC), which is easily accessible to oxygen during its combustion, activated by these Ni particles.

ii) Coke deposited on Ni-La_2O_3 and/or Ni-Al_2O_3 interface (peak at 420 ºC), whose gasification is enhanced by La_2O_3 and thus its content decreases markedly by increasing temperature above 600 °C (Fig. 10) and by increasing space-time (Fig. 11). Consequently, it is almost undetectable at 700 °C with high value of space-time (Fig. 11b).

iii) Coke deposited on α-Al_2O_3 support (peak at 620-660 ºC), whose combustion is not catalytically activated and may even be hindered by oxygen diffusional limitation within the porous structure of this α-Al_2O_3.

These hypotheses are supported by studies in literature that highlight the interest of studying TPO profiles to analyze the coke nature and its location for different catalytic processes [33-37].

3.3.2. Coke formation mechanism

Based on the scheme in Fig. 7, bio-oil oxygenates are considered coke formation precursors, and so oxygenates concentration in the reaction medium is higher as the reforming activity decreases (step 1), which contributes to producing more coke (step 2). This effect, which explains the evolution of product distribution with time on stream, is typical in catalytic processes in which deactivation occurs in parallel with the main reaction and has been studied in reactions of hydrocarbon production from pure oxygenates (methanol and ethanol) [38,39] and from bio-oil [33,40,41].

Understanding of the effect of operating conditions on the content and properties of coke

requires consideration of the steps involved in the formation and evolution of this coke. These steps were already discussed by Yung et al. [42] and they have been included in the scheme of Fig. 12. In this scheme there are a stabilization step of the active precursor (C*, adsorbed on the metal sites of the catalyst) to form coke (C* + C* $\rightarrow$ coke) and the C* intermediates are also transformed into gaseous products by other reactions: Boudouard reaction (C* + $CO_2 \Leftrightarrow 2CO$), gasification (C* + $H_2O \rightarrow CO + H_2$) and methanation (C* + $2H_2 \Leftrightarrow CH_4$). These reactions, of coke formation and removal, are additional to the reforming of bio-oil oxygenates and their relative importance and thermodynamic equilibrium depend on the operating conditions.

Figure 12

The byproducts are partially transformed (by reforming or WGS reaction) when the catalyst has enough activity. However, as catalyst undergoes deactivation for the reforming reactions, other secondary reactions (step 3) are enhanced and produce CO, CH_4 and hydrocarbons. These byproducts are potential reactants under these conditions for the formation of precursors (C *) and for coke formation by the reactions shown in Fig. 12.

The transformation of coke precursors (C*) into gases is obviously enhanced by the reactivity of C* (higher as it is more hydrogenated) and by the concentration of CO_2, H_2O and H_2 in the reaction medium. Consequently, from the perspective of minimizing the deactivation by coke, the catalyst composition and reaction conditions should favour the transformation of this carbonaceous material C* into gases, and should minimize its stabilization to form less active or inactive coke. Accordingly, the formation of C-O active bonds should be promoted, which minimizes C-C bond formation by joining two C*. These undesired steps of coke formation and development are enhanced by higher temperature, but this increase also favours the carbonaceous material (C*) gasification due to the high steam concentration in the reaction medium. Consequently, as it was proven by the results of previous sections, temperature is the most important variable in order to minimize deactivation by coke in the bio-oil aqueous fraction reforming.

Furthermore, although Ni particles in the catalyst are active to form both types of bonds, there are certain factors, such as Ni particle size decrease or the incorporation of promoters (such as La_2O_3), which contribute to attenuating: i) C-C bond formation; ii) blockade of

metal particles, iii) release and subsequent dragging of these particles by the coke nanotubes growing outwards the catalyst particles.

3.4. Deactivation of catalyst by metal sintering

The results of the average Ni crystal size analyzed by XRD of the deactivated catalysts in the 600-800 °C range are shown in Table 4. There is a significant sintering above 800 °C and thereby the crystal size is three times higher in the deactivated catalyst with respect to the fresh.

Table 4

With the aim of studying in more detail the joint effect of temperature and water content in the reaction medium on Ni sintering, hydrothermal treatment experiments were carried out at three temperatures (600, 700 and 800 °C) and two water flowrates (0.035 and 0.5 ml/min). The experiments were performed with a bed of 0.5 g of catalyst and 2 g of CSi, and H_2 flow of 10 ml/min (in order to simulate actual conditions of the reaction streams). The treatment time was 10 h in all experiments. Table 5 shows the results of Ni crystal size after the treatment. It can be noted that Ni sintering is very important at 800 °C, whereas is appreciable at 700 °C when water content is very high (much higher than the reaction conditions) and it is negligible at 600 °C. Consequently, water content has a significant effect on Ni sintering above 700 °C.

Table 5

Fig. 13 shows the XRD diffractograms of the catalyst samples that have undergone sintering. It is worth noting the result of sample *d* (catalyst subjected to 800 °C and water stream of 0.5 ml/min), where the peak at 37.5° increases and the peak at 67° shifts slightly to the left. These peaks correspond to nickel aluminate, $Ni(Al_2O_4)$, which is a not very active material for the reforming [43].

Figure 13

The result of 700 °C as suitable temperature for reforming the aqueous fraction of bio-oil (since above this temperature Ni sintering is remarkable) is consistent with other results in the literature for Ni/Al_2O_3 catalysts [44-46].

3.5. Comparison of different catalysts and technologies

Table 6 shows a comparative summary of the literature results obtained in the bio-oil aqueous fraction reforming. The results are different since they correspond to catalysts with different composition and obtained by using fixed bed, fluidized and spouted bed reactors. Besides, they were obtained with very different values of space-time, and the information provided about the catalysts stability is limited.

Apart from the high H_2 yield, the two-step process used in this work has other advantages, mainly the avoidance of the operational problems caused by pyrolytic lignin deposition and a negligible deactivation of the catalyst under the suitable conditions. The main difference with the single step reaction is that a fraction of bio-oil oxygenates (30 wt%) is transformed into pyrolytic lignin, so that H_2 production is 42 mol $(kg_{bio\text{-}oil})^{-1}$. Medrano et al. [12] obtained 60 mol $(kg_{bio\text{-}oil})^{-1}$ in one-step reaction, and therefore a study on the valorisation of pyrolytic lignin will be interesting in order to improve the viability of the two-step process studied in this work.

Table 6

4. Conclusions

The process with two steps in series (thermal-catalytic) is effective for reforming the aqueous fraction of bio-oil in a continuous regime since it avoids operational problems and catalyst deactivation. These drawbacks are inherent in the repolymerization in the reactor of derivatives of the lignin contained in bio-oil.

The $Ni/La_2O_3\text{-}\alpha Al_2O_3$ catalyst is highly stable, with a high capacity for reforming coke precursors and high resistance to sintering, with both properties being attributed to the presence of La_2O_3.

Based on the content and properties of the coke and its effect on deactivation, this has a heterogeneous composition due to its deposition in different catalyst locations (Ni metal particles, $Ni\text{-}La_2O_3$ and/or $Ni\text{-}Al_2O_3$ interface and $\alpha\text{-}Al_2O_3$ support). Furthermore, coke deposition is highly dependent on operating conditions (particularly temperature).

The effect of operating conditions on deactivation by coke was explained considering the reactions involved in coke formation and transformation into gaseous products.

Consequently, the reforming temperature is a key factor for minimizing catalyst deactivation, with 650-700 °C being the suitable range, because coke gasification is enhanced without sintering of Ni. At 700 °C and space-time of 0.45 $g_{catalyst}\ h(g_{bio\text{-}oil})^{-1}$ bio-oil oxygenates are fully converted, and a H_2 yield of 95 % and a H_2 selectivity of 70 % are achieved. Under these conditions the catalyst remains stable during 5 h.

Acknowledgments

This work was carried out with the financial support of the Department of Education Universities and Investigation of the Basque Government (Project GIC07/24-IT-220-07), of the University of the Basque Country (UFI 11/39) and of the Ministry of Science and Innovation of the Spanish Government (Project CTQ2009-13428/PPQ).

Nomenclature

C*	Carbonaceous material adsorbed on the metal sites of the catalyst
C_C	Coke content, wt %
C_{H2}	Hydrogen concentration, vol %
d_M	Average diameter of Ni metal particle, nm
$F_{bio\text{-}oil,}$	Molar flow rate of bio-oil, in dry basis, mol h^{-1}
$G_{C1}HSV$	Gas hourly space velocity, defined in equivalent CH_4 units, h^{-1}
Y_{H2}	Hydrogen yield for the reforming step, expressed as percentage of the stoichiometric maximum, %
Y_i	*i* carbonaceous product yield, in units of carbon fed, mol *i* (mol C fed)$^{-1}$
P_{H2}	Hydrogen productivity, mmol·$(g_{bio\text{-}oil})^{-1}$
S/C	Steam to (carbon in the bio-oil) ratio fed to the reactor
S_{H2}	Hydrogen selectivity, %
T	Temperature, ºC.
X	Bio-oil conversion
τ	Space-time, $g_{catalyst}h(g_{bio\text{-}oil})^{-1}$.

References

[1] A. Demirbas, Biohydrogen for future engine fuel demands, Springer, London, 2009.

[2] E. Kirtay, Recent advances in production of hydrogen from biomass, Energy Conver. Manage. 52 (2011) 1778-1789.

[3] H. Balat, E. Kirtay, Hydrogen from biomass-Present scenario and future prospects, Int. J. Hydrogen Energy 35 (2010) 7416-7426.

[4] H. Qinglan, W. Chang, L.Y. Dingqiang, L. Dan, L. Guiju, Production of hydrogen-rich gas from plant biomass by catalytic pyrolysis at low temperature, Int. J. Hydrogen Energy 35 (2010) 8884-8890.

[5] H.C. Yoon, T. Cooper, A. Steinfeld, Non-catalytic autothermal gasification of woody biomass, Int. J. Hydrogen Energy 36 (2011) 7852-7860.

[6] B. Acharya, A. Dutta, P. Basu, An investigation into steam gasification of biomass for hydrogen enriched gas production in presence of CaO, Int. J. Hydrogen Energy 35 (2010) 1582-1589.

[7] E. Butler, G. Devlin, D. Meier, K. McDonnell, A review of recent laboratory research and commercial developments in fast pyrolysis and upgrading, Renew. Sust. Energy Rev. 15 (2011) 4171-4186.

[8] A.G. Gayubo, A.T. Aguayo, A. Atutxa, R. Prieto, J. Bilbao, Deactivation of a HZSM-5 catalyst in the transformation of the aqueous fraction of biomass pyrolysis-oil into hydrocarbons, Energy Fuels 18 (2004) 1640-1647.

[9] D. Wang, S. Czernik, E. Chornet, Energy Fuels 12 (1998) 19-24.

[10] T. Chen, C. Wu, R. Liu, Steam reforming of bio-oil from rice husks fast pyrolysis for hydrogen production, Bioresour. Technol. 102 (2011) 9236-9240.

[11] H. Li, Q. Xu, H. Xue, Y. Yan, Catalytic reforming of the aqueous phase derived from fast-pyrolysis of biomass, Renew. Energy 34 (2009) 2872-2877.

[12] J.A. Medrano, M. Oliva, J. Ruiz, L. García, J. Arauzo, Hydrogen from aqueous fraction of biomass pyrolysis liquids by catalytic steam reforming in fluidized bed, Energy 36 (2011) 2215-2224.

[13] S. Zhang, X. Li, Q. Xu, Y. Yan, Hydrogen production from the aqueous phase derived from fast pyrolysis of biomass, J. Anal. Appl. Pyrolysis 92 (2011) 158-163.

[14] P.N. Kechagiopoulos, S.S. Voutetakis, A.A. Lemonidou, I.A. Vasalos, Hydrogen production via reforming of the aqueous phase of bio-oil in a fixed bed reactor, Energy Fuels 20 (2006) 2155-2163.

[15] A.C. Basagianis, X.E. Verykios, Steam reforming of the aqueous fraction of bio-oil over structured $Ru/MgO/Al_2O_3$ catalysts, Catal. Today 127 (2007) 256-264.

[16] P.N. Kechagiopoulos, S.S. Voutetakis, A.A. Lemonidou, I.A. Vasalos, Hydrogen production via reforming of the aqueous phase of bio-oil over Ni/olivine catalysts in a spouted bed reactor, Ind. Eng. Chem. Res. 48 (2009) 1400-1408.

[17] G. van Rossum, S.R.A. Kersten, W.P.M. van Swaaij, Catalytic and Noncatalytic Gasification of Pyrolysis Oil, Ind. Eng. Chem. Res. 46 (2007) 3959-3967.

[18] S. Czernik, R. French, C. Feik, E. Chornet, Hydrogen by catalytic steam reforming of liquid byproducts from biomass thermoconversion processes, Ind. Eng. Chem. Res. 41 (2002) 4209-4215.

[19] C.F. Yan, E.Y. Hu, C.L. Cai, Hydrogen production from bio-oil aqueous fraction with in situ carbon dioxide capture, Int. J. Hydrogen Energy 35 (2010) 2612-2616.

[20] B. Valle, A. Remiro, M. Olazar, A.G. Gayubo, J. Bilbao, Catalysts of Ni/α-Al_2O_3 and Ni/La_2O_3-αAl_2O_3 for hydrogen production by steam reforming of bio-oil aqueous fraction with pyrolytic lignin retention, Int. J. Hydrogen Energy 38 (2013) 1307-1318.

[21] J. Makibar, A.R. Fernandez-Akarregi, I. Alava, F. Cueva, G. Lopez, M. Olazar, Investigations on heat transfer and hydrodynamics under pyrolysis conditions of a pilot-plant draft tube conical spouted bed reactor, Chem. Eng. Process.: Process Inten. 50 (2012) 790-798.

[22] M. Amutio, G. López, M. Artetxe, G. Elordi, M. Olazar, J. Bilbao, Influence of temperature on biomass pyrolysis in a conical spouted bed reactor, Resour. Conserv. Recycling 59 (2012) 23-31.

[23] M. Amutio, G. Lopez, R. Aguado, J. Bilbao, M. Olazar, Biomass oxidative flash pyrolysis: autothermal operation, yields and product properties, Energy Fuels 26 (2012) 1353-1362.

[24] A.L. Alberton, M.M.V.M. Souza, M. Schmal, Carbon formation and its influence on ethanol steam reforming over Ni/Al_2O_3 catalysts, Catal. Today 123 (2007) 257-264.

[25] C. Li, Y.W. Chen, Temperature-programmed-reduction studies of nickel oxide/alumina catalysts: effects of the preparation method, Thermochim. Acta 256 (1995) 457-465.

[26] M.C. Sánchez-Sánchez, R.M. Navarro, J.L.G. Fierro, Ethanol steam reforming over Ni/La-Al_2O_3 catalysts: Influence of lanthanum loading, Catal. Today 129 (2007) 336-345.

[27] A.G. Gayubo, B. Valle, A.T. Aguayo, M. Olazar, J. Bilbao, Pyrolytic lignin removal for the valorisation of biomass pyrolysis crude bio-oil by catalytic transformation, J. Chem. Tech. Biotechnol. 85 (2010) 132-144.

[28] A. G. Gayubo, B. Valle, A.T. Aguayo, M. Olazar, J. Bilbao, Olefin production by catalytic transformation of crude bio-oil in a two-step process, Ind. Eng. Chem. Res. 49 (2010) 123-131.

[29] B. Valle, A.G. Gayubo, A.T. Aguayo, M. Olazar, J. Bilbao, Selective production of aromatics by crude bio-oil valorization with a Ni modified HZSM-5 catalyst, Energy Fuels 24 (2010) 2060-2070.

[30] E. Ch. Vagia, A.A. Lemonidou, Hydrogen production via steam reforming of bio-oil components over calcium aluminate supported nickel and noble metal catalysts, Appl. Catal. A: General 351 (2008) 111-121.

[31] W. Wang, R. Ran, Z. Shao, Lithium and lanthanum promoted Ni-Al_2O_3 as an active and highly coking resistant catalyst layer for solid-oxide fuel cells operating on methane, J. Power Sources 196 (2011) 90-97.

[32] V.R. Choudary, S. Banerjee, A.M. Rajput, Continuous Production of H_2 at Low Temperature from Methane Decomposition over Ni-Containing Catalyst Followed by Gasification by Steam of the Carbon on the Catalyst in Two Parallel Reactors Operated in Cyclic Manner, J. Catal. 198 (2001) 136-141.

[33] B. Valle, P. Castaño, M. Olazar, J. Bilbao, A.G. Gayubo, Deactivating species in the transformation of crude bio-oil with methanol into hydrocarbons on a HZSM-5 catalyst, J. Catal. 285 (2012) 304-314.

[34] I. Sierra, J. Ereña, A.T. Aguayo, M. Olazar, J. Bilbao, Regeneration of CuO-ZnO-Al_2O_3/γ-Al_2O_3 catalyst in the direct synthesis of dimethyl ether, Appl. Catal. B: Environmental 94 (2010) 108-116.

[35] P. Castaño, G. Elordi, M. Olazar, A.T. Aguayo, B.G. Pawelec, J. Bilbao, Insights into the coke deposited on HZSM-5, Hβ and HY zeolites during the cracking of polyethylene, Appl. Catal B: Environmental 104 (2011) 91-100.

[36] P. Castaño, A. Gutiérrez, I. Hita, J.M. Arandes, A.T. Aguayo, J. Bilbao, Deactivating species deposited on Pt-Pd catalysts in the hydrocracking of light cycle oil, Energy Fuels 26 (2012) 1509-1519.

[37] J. Ereña, I. Sierra, M. Olazar, A.G. Gayubo, A.T. Aguayo, Deactivation of a CuO-ZnO-Al_2O_3/gamma-Al_2O_3 catalyst in the synthesis of dimethyl ether, Ind. Eng. Chem. Res. 47 (2008) 2238-2247.

[38] A.T. Aguayo, P. Castaño, D. Mier, A.G. Gayubo, M. Olazar, J. Bilbao, Effect of Cofeeding Butane with Methanol on the Deactivation by Coke of a HZSM-5 Zeolite Catalyst, Ind. Eng. Chem. Res. 50 (2011) 9980-9988.

[39] A. G. Gayubo, A. Alonso, B. Valle, A.T. Aguayo, J. Bilbao, Selective production of olefins from bioethanol on HZSM-5 zeolite catalysts treated with NaOH, Appl. Catal. B: Environmental 97 (2010) 299-306.

[40] A.G. Gayubo, A.T. Aguayo, A. Atutxa, B. Valle, J. Bilbao, Undesired components in the transformation of biomass pyrolysis oil into hydrocarbons on an HZSM-5 zeolite catalyst, J. Chem. Tech. Biotechnol. 80 (2005) 1244-1251.

[41] A.G. Gayubo, B. Valle, A.T. Aguayo, M. Olazar, J. Bilbao, Attenuation of catalyst deactivation by cofeeding methanol for enhancing the valorisation of crude bio-oil, Energy Fuels 23 (2009) 4129-4136.

[42] M.M. Yung, W.S. Jablonski, K.A. Magrini-Bair, Review of catalytic conditioning of biomass derived syngas, Energy Fuels 23 (2009) 1874-1887

[43] J.R. Rostrup-Nielsen in J.R. Anderson and M. Boudart (Eds.). Catalysis, Science and Technology, 1984. Springer-Verlag.

[44] J. Sehested, Sintering of nickel steam-reforming catalysts, J. Catal. 217 (2003) 417-426.

[45] F.B. Rasmussen, J. Sehested, H.T. Teunissen, A.M. Molenbroek, B.S. Clausen, Sintering of Ni/Al_2O_3 catalysts studied by anomalous small angle X-ray scattering, Appl. Catal. A: General 267 (2004) 165-173.

[46] J. Sehested, J.A.P. Gesten, I.N. Remediakis, H. Bengaard, J.K. Nørskov, Sintering of nickel steam-reforming catalysts: effects of temperature and steam and hydrogen pressures, J. Catal. 223 (2004) 432-443.

[47] L. Garcia, R. French, S. Czernik, E. Chornet, Catalytic steam reforming of bio-oils for the production of hydrogen: Effects of catalyst composition, Appl. Catal. A: General 201 (2000) 225-239.

[48] Q. Xu, P. Lan, B. Zhang, Z. Ren, Y. Yan, Hydrogen Production via Catalytic Steam Reforming of Fast Pyrolysis Bio-oil in a Fluidized-Bed Reactor, Energy Fuels 24 (2010) 6456-6462.

Figure Captions

Fig. 1. Two-step (thermal-catalytic) process for bio-oil steam reforming.

Fig, 2. Scheme of reaction equipment.

Fig. 3. Effect of temperature on the evolution with time on stream of bio-oil aqueous fraction conversion. Conditions: τ = 0.22 $g_{catalyst}h(g_{bio\text{-}oil})^{-1}$, S/C = 12, 500-800 ºC ($G_{C1}HSV$ = 12800-17800 h^{-1}).

Fig. 4. Effect of temperature on the evolution with time on stream of H_2 yield and selectivity (a), CO and CO_2 yields (b), CH_4 and hydrocarbons yields (c). Conditions: τ = 0.22 $g_{catalyst}h(g_{bio\text{-}oil})^{-1}$, S/C = 12, 500-800 ºC ($G_{C1}HSV$ = 12800-17800 h^{-1}).

Fig. 5. Effect of space-time on the evolution with time on stream of bio-oil aqueous fraction conversion. Conditions: 700 ºC, S/C = 12, $G_{C1}HSV$ = 40300, 16100, 8100 h^{-1}.

Fig. 6. Effect of space-time on the evolution with time on stream of H_2 yield and selectivity (a), CO and CO_2 yields (b), CH_4 and hydrocarbons yields (c). Conditions: 700 ºC, S/C = 12, $G_{C1}HSV$ = 40300, 16100, 8100 h^{-1}.

Fig. 7. Reaction steps of bio-oil steam reforming in the 500-800 ºC range.

Fig. 8. Effect of temperature and space-time on the evolution with time on stream of bio-oil aqueous fraction conversion. Conditions: 600-700 ºC, S/C = 12, τ = 0.10-0.45 $g_{catalyst}h(g_{bio\text{-}oil})^{-1}$ ($G_{C1}HSV$ = 40300-8100 h^{-1}).

Fig. 9. Effect of temperature and space-time on the evolution with time on stream of H_2 yield (a), CO and CO_2 yields (b), CH_4 and hydrocarbons yields (c). Conditions: 600-700 ºC, S/C = 12, τ = 0.10-0.45 $g_{catalyst}h(g_{bio\text{-}oil})^{-1}$ ($G_{C1}HSV$ = 40300-8100 h^{-1}).

Fig. 10. Comparison of TPO profiles for different reaction temperatures (500, 550, 650ºC). Conditions: S/C = 12, τ = 0.22 $g_{catalyst}h(g_{bio\text{-}oil})^{-1}$, reaction time = 5 h.

Fig. 11. Effect of space-time on TPO profiles for reaction temperatures 600 ºC (a) and 700 ºC (b). Conditions: S/C = 12, τ = 0.1 and 0.45 $g_{catalyst}h(g_{bio\text{-}oil})^{-1}$, reaction time = 5 h.

Fig. 12. Routes of coke evolution in the catalytic steam reforming over metal catalysts.

Fig. 13. Effect of hydrothermal treatment (10 h) on XRD spectra of Ni/La_2O_3-αAl_2O_3 catalyst: a) 700 ºC, 0.035 ml min^{-1}, b) 700 ºC, 0.5 ml min^{-1}, c) 800 ºC, 0.035 ml min^{-1}, d) 800 ºC, 0.5 ml min^{-1}.

TABLES

Table 1. Mass composition and molecular formula of the crude bio-oil and the aqueous fraction.

Compound	Bio-oil	Aqueous fraction
Acetic acid	12.8	19.1
Acetone	5.5	1.0
Formic acid	2.1	2.7
Methanol	1.3	1.0
1-hydroxy-2-propanone	16.3	8.7
Hydroxyacetaldehyde	8.5	1.8
Levoglucosane	11.0	19.6
Hexose	1.9	2.7
Other ketones	3.8	8.1
Other acids	1.9	4.7
Esters	5.1	3.1
Other aldehydes	6.5	5.5
Phenols	16.6	13.4
Ethers	1.4	0.3
Alcohols	2.4	3.6
Others	2.9	4.7
Molecular formula	$C_{4.3}H_{7.2}O_{2.6}$	$C_{4.1}H_{7.4}O_{2.7}$

Table 2. Effect of reforming temperature on coke contents and TPO profiles after 5 h of reaction. Conditions: S/C = 12, τ = 0.22 $g_{catalyst}\,h(g_{bio\text{-}oil})^{-1}$, GHSV= 12800-17800 h^{-1}.

T, ºC	Results of TPO		
	C_c, wt %	peaks	ºC
500	3.3	4	290 354 416 490
550	1.3	5	291 351 422 493 610
600	0.9	3	286 349 612
650	0.5	3	282 350 615
700	0.3	3	286 489 610
800	0	0	-

Table 3. Effect of reforming temperature and space-time on coke contents after 5 h of reaction.

T, ºC	Space-time, $g_{catalyst}h(g_{bio\text{-}oil})^{-1}$	C_c, wt% g_{coke}/(100 g catalyst)	Coke yield, wt% g_{coke}/(100 g C in the fed)
600	0.45	0.5	0.142
	0.1	3.4	0.193
700	0.45	0.2	0.067
	0.1	1.3	0.075

Table 4. Effect of reforming temperature on Ni metal sintering after 5 h of reaction for space-time (τ) = 0.22 $g_{catalyst}h(g_{bio\text{-}oil})^{-1}$.

T, ºC	d_m Niº, nm
600	12.0
700	14.7
800	39.9
Fresh catalyst	11.9

Table 5 Effect of different hydrothermal conditions on Ni metal sintering after 10 h of treatment for space-time (τ) = 0.22 $g_{catalyst}h(g_{bio\text{-}oil})^{-1}$.

Conditions		d_M Ni^0, nm
T, ºC	Q_{H2O}, ml $(min)^{-1}$	
600 ºC	0.035	12.0
600 ºC	0.5	12.0
700 ºC	0.035	13.3
700 ºC	0.5	23.8
800 ºC	0.035	23.9
800 ºC	0.5	-
Fresh catalyst (reduced at 700 ºC)		11.9

Table 6. Production of hydrogen by steam reforming of the aqueous fraction of bio-oil with different catalysts and technologies.

Reference	Reactor	Metal	Support	T,ºC	S/C	GHSV, h^{-1}	C_{H2}, % vol	P_{H2}, $mmol/g_{bio-oil}$	Y_{H2}, %
[46]	Fixed bed (microreactor)	Ni-K-Mg	Al_2O_3-CaO[(a)]	825	4.92	126000	-	-	87
		Ni (15 %) Co (5 %)	MgO-La_2O_3-Al_2O_3	825	4.92	62300	-	-	90
[17]	Fluidized bed	Ni-K-Mg	Al_2O_3-CaO[(a)]	850	9.0	830	-	15	89
[16]	Spouted bed	Ni (5 %)	olivine	850	5.37	-	48	-	43
[11]	Fluidized bed	Ni (20 %)	Dolomite[(b)]	800	5	1.5[(c)]	-	-	72
[47]	Fluidized bed	Ni (7.2 %)	MgO	700	17	0.4[(c)]	60	-	56
[18]	Fixed bed	Ni (12 %)	CeO_2-ZrO_2	800	4.9	-	61.9	-	69.7
		Ni	Z417[(d)]	800	4.9		59.8		60
[12]	Fluidized bed	Ni (28 %) Mg (3 %)	Al_2O_3	650	7.64	5411	67.4	60	70
[10]	Fixed bed	Ni	--[(e)]	850	15	0.3[(c)]	-	-	45.3
[13]	Fluidized bed	Ni (7.2 %)	MgO	800	10	1.0[(c)]	-	-	64.6
Present work	Fluidized bed	Ni (10 %)	La_2O_3-αAl_2O_3	700	12	4700/14[(c)]	71	41.8	95[(f)]/84[(g)]

(a) C11-NK, commercial catalyst for nafta reforming
(b) Dolomite modified with $Mg(NO_3)_2$
(c) WHSV, h^{-1}
(d) Commercial Ni catalyst, Z417
(e) Commercial Ni catalyst
(f) Yield in the reforming reactor
(g) Overall yield in two-step system

FIGURES

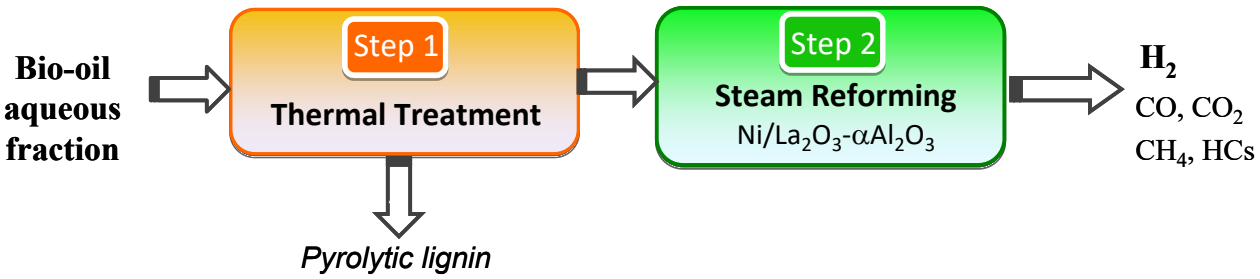

Figure 1

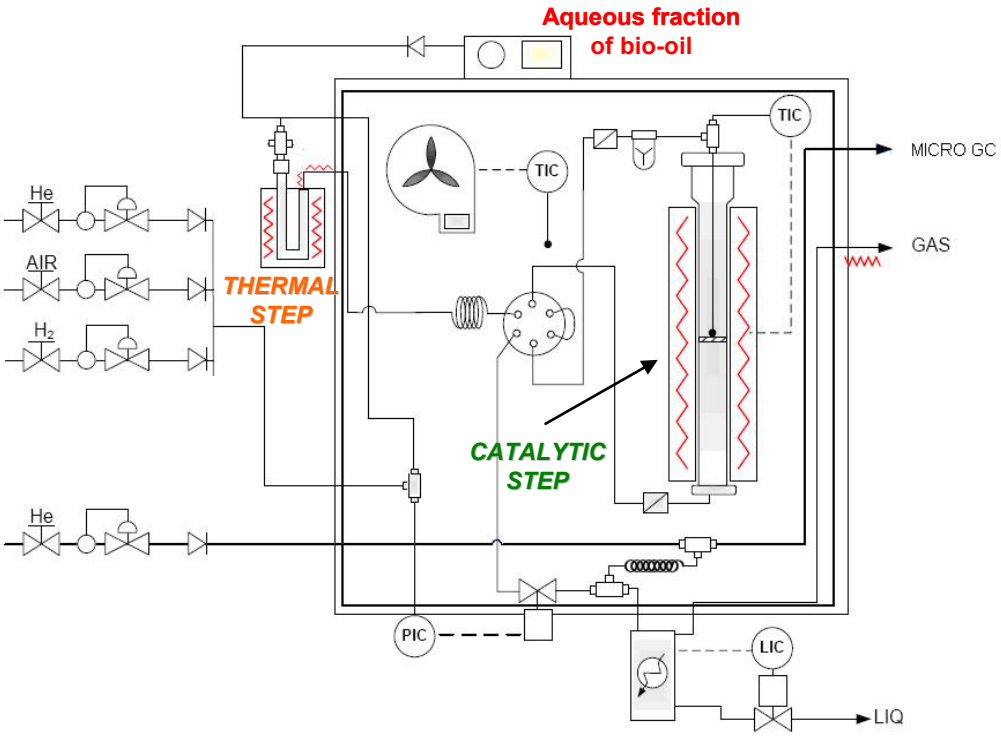

Figure 2

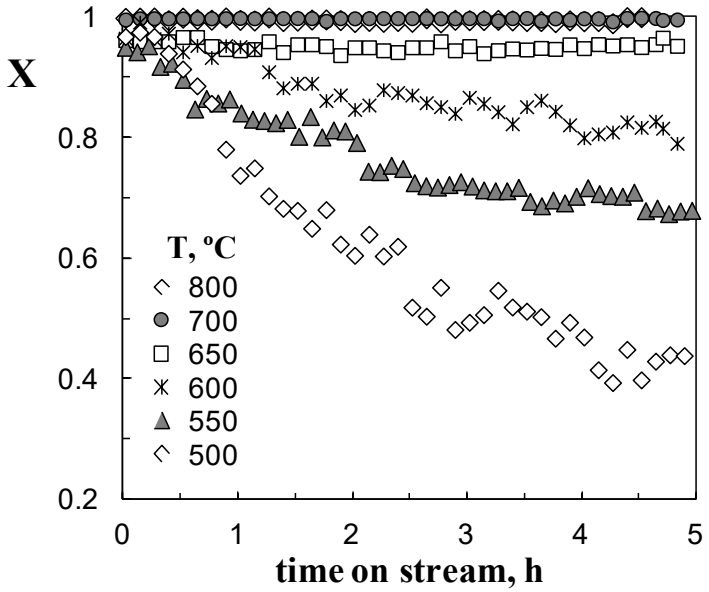

Figure 3

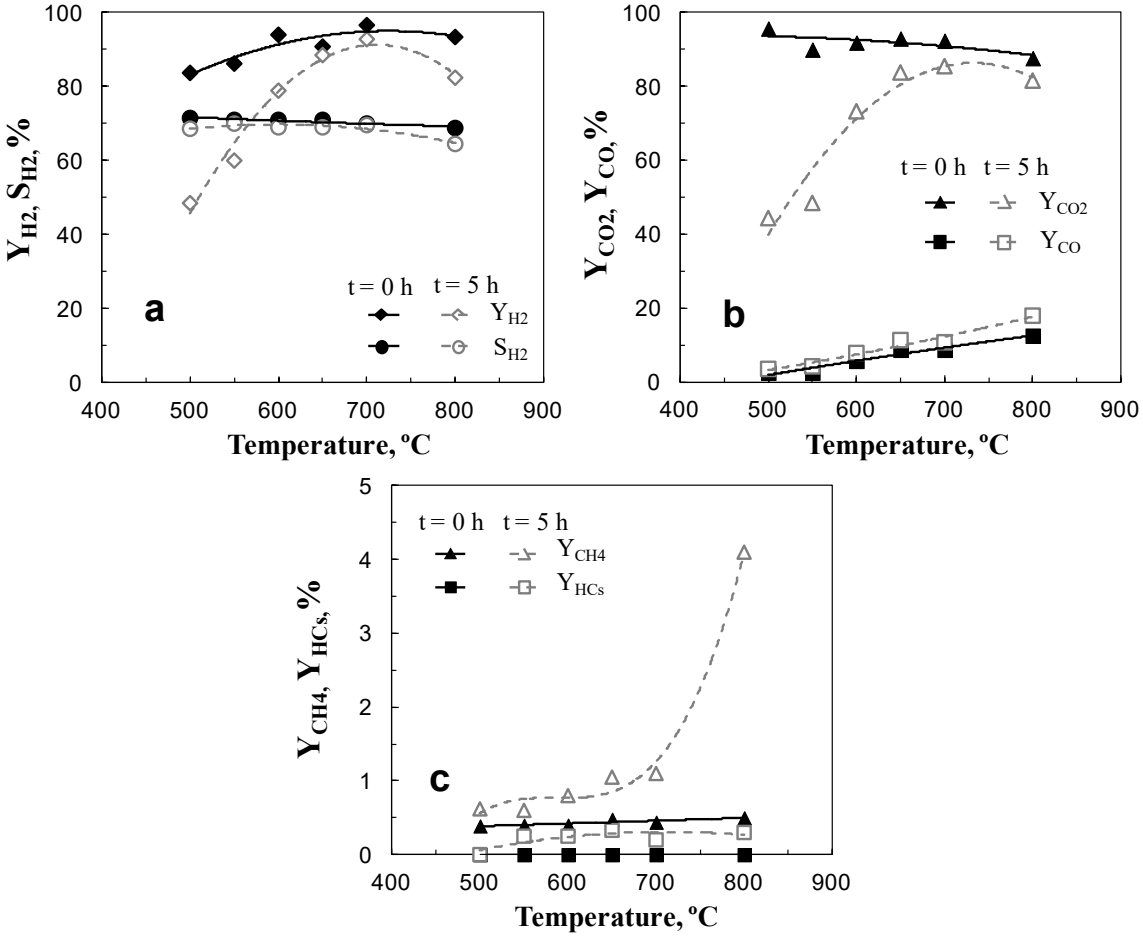

Figure 4

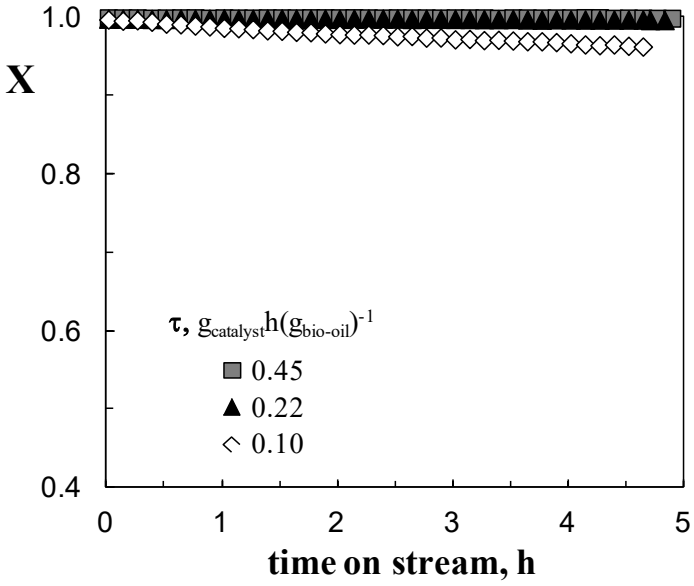

Figure 5

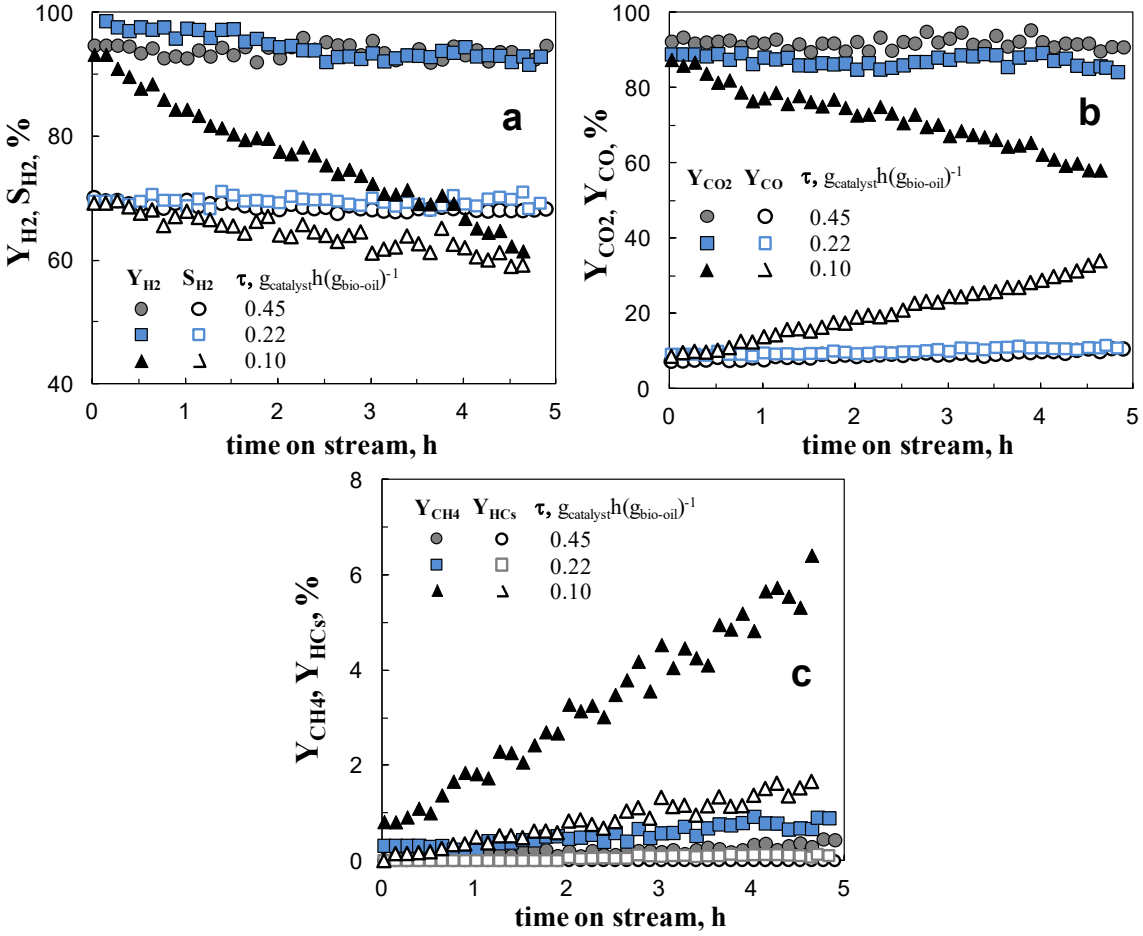

Figure 6

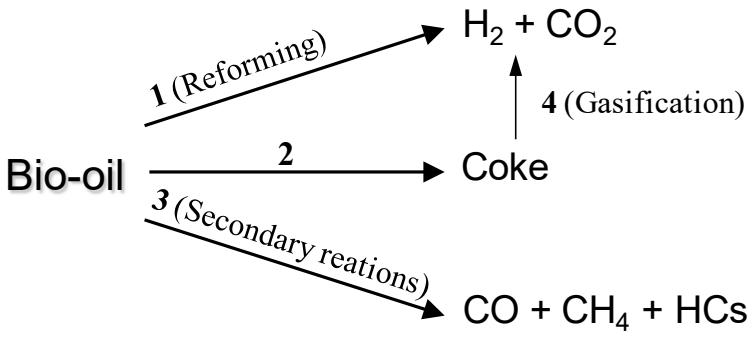

Figure 7

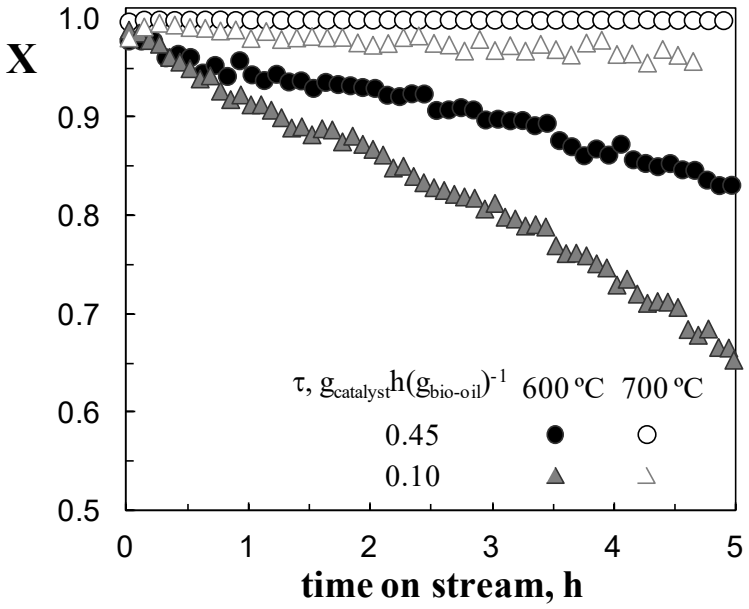

Figure 8

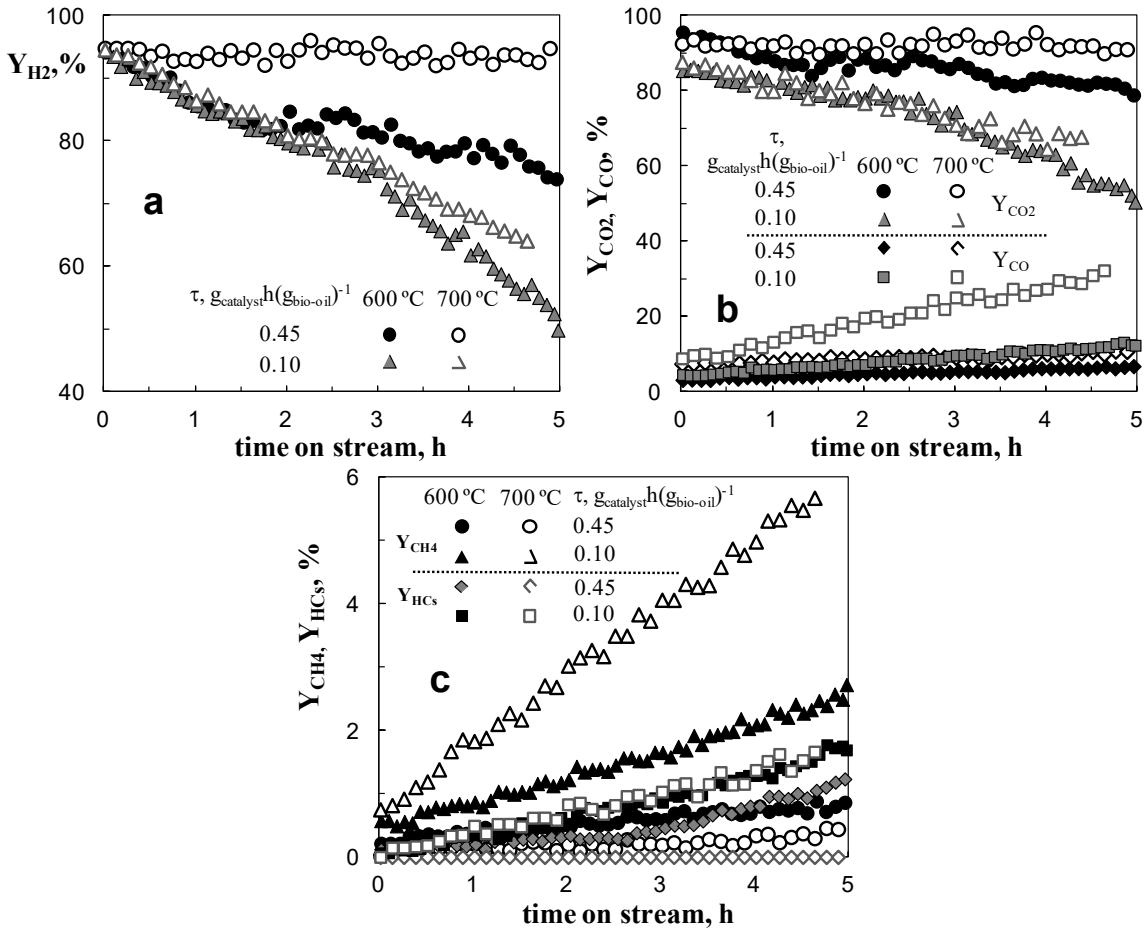

Figure 9

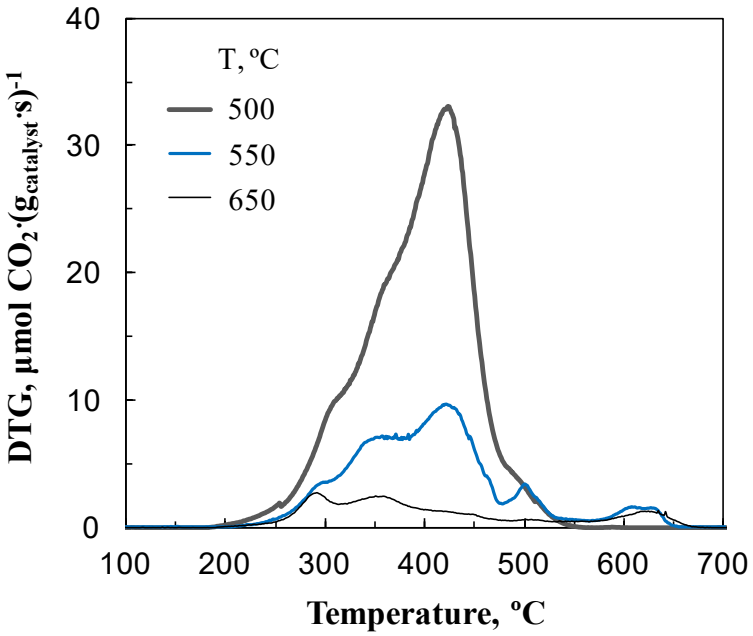

Figure 10

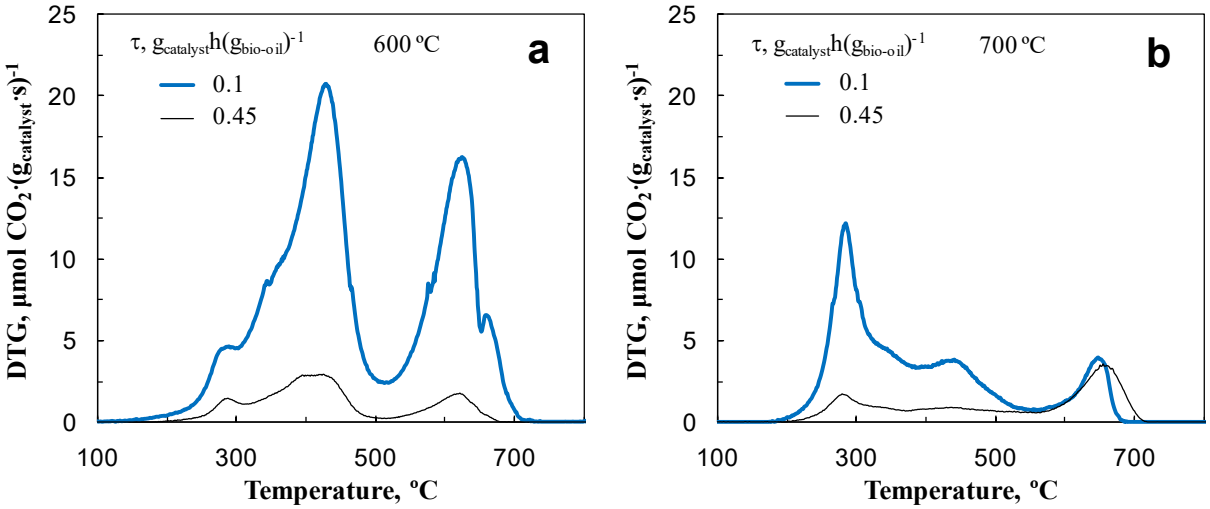

Figure 11

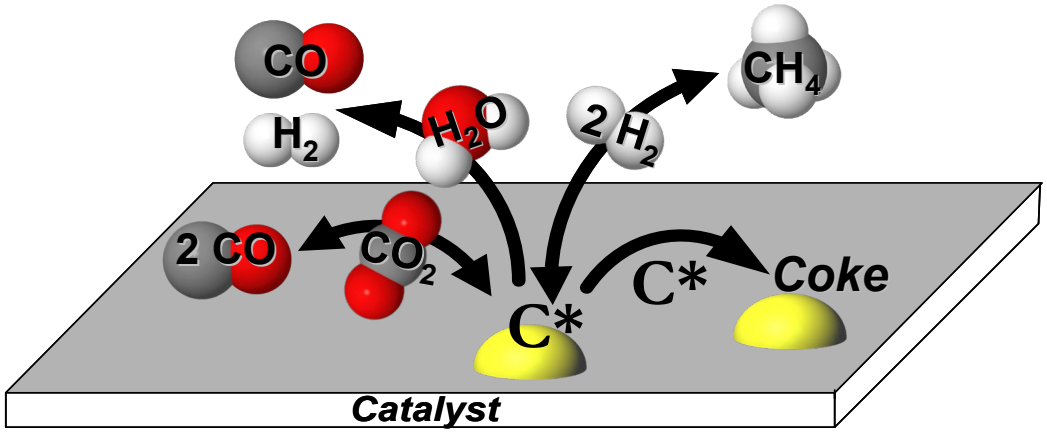

Figure 12

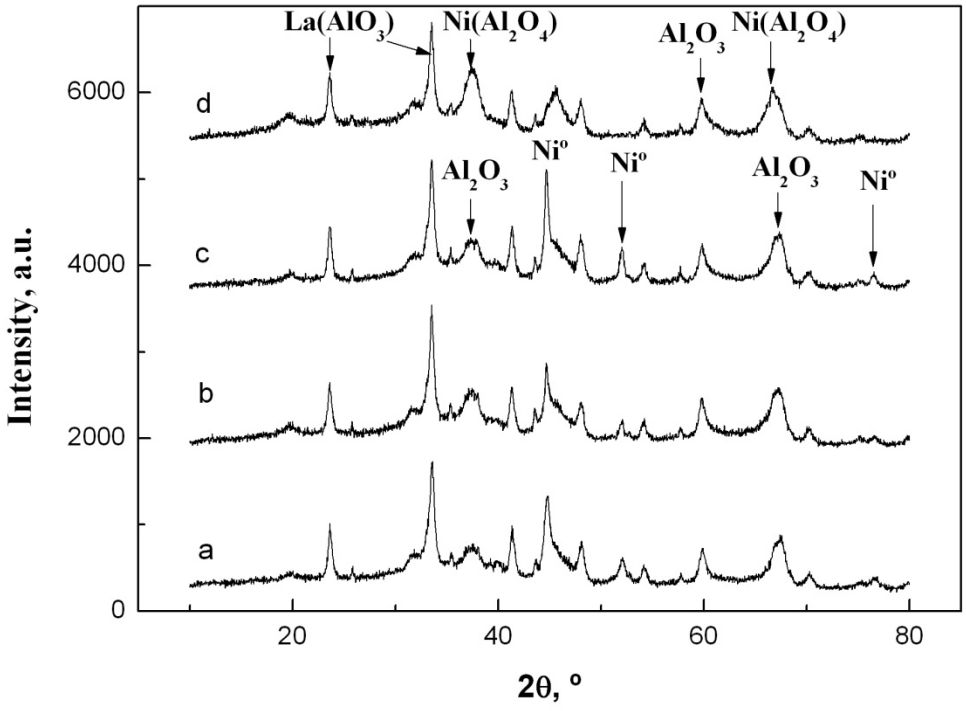
La(AlO3)
Ni(Al2O4)
Al2O3
Ni(Al2O4)
Ni°
Al2O3
Ni°
Al2O3
Ni°
d
c
b
a
Intensity, a.u.
2θ, °
0
2000
4000
6000
20
40
60
80

Figure 13